### **WATER STRUCTURE**

# Deconstructing water's diffuse OH stretching vibrational spectrum with cold clusters

Nan Yang<sup>1</sup>, Chinh H. Duong<sup>1</sup>, Patrick J. Kelleher<sup>1</sup>, Anne B. McCoy<sup>2\*</sup>, Mark A. Johnson<sup>1\*</sup>

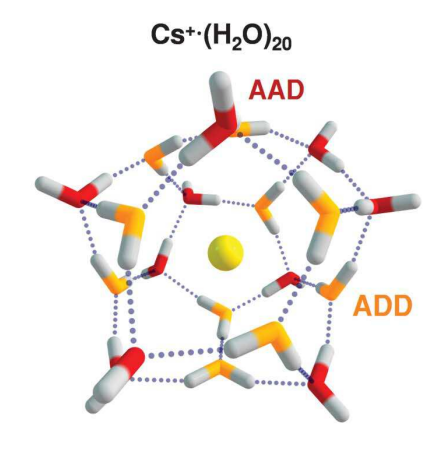
The diffuse vibrational envelope displayed by water precludes direct observation of how different hydrogen-bond topologies dictate the spectral response of individual hydroxy group (OH) oscillators. Using cold, isotopically labeled cluster ions, we report the spectral signatures of a single, intact water ( $H_2O$ ) molecule embedded at various sites in the clathrate-like cage structure adopted by the  $Cs^+\cdot(D_2O)_{2O}$  ion. These patterns reveal the site-dependent correlation between the frequencies of the two OH groups on the same water molecule and establish that the bound OH companion of the free OH group exclusively accounts for bands in the lower-energy region of the spectrum. The observed multiplet structures reveal the homogeneous linewidths of the fundamentals and quantify the anharmonic contributions arising from coupling to both the intramolecular bending and intermolecular soft modes.

nderstanding the transient local structures and ultrafast dynamics that account for the broad vibrational envelope displayed by water in the OH stretching region is a challenge for contemporary physical chemistry (1-3). A common ansatz, for example, posits that, if the local network surrounding a single OH group could be frozen in place, that oscillator would yield a single absorption feature at a frequency determined by the H-bonding configurations of the neighboring water molecules (4, 5). The envelope of the observed spectrum can then be recovered by invoking rapid "spectral diffusion" arising from the thermal fluctuations in the network structure that rapidly move this transition across the spectrum (6, 7). In isotopically homogeneous water, this process is masked by the delocalized nature of the vibrational excitation among nearby, nominally equivalent OH groups (i.e., vibrational excitons) (8, 9). Although this complication can be overcome by diluting H<sub>2</sub>O in excess D<sub>2</sub>O, which yields a sample where the OH groups are dominated by HDO and are thus decoupled from the surrounding array of OD oscillators (10), the resulting OH spectrum is still quite diffuse. Here, we are concerned with the related situation in which a single, intact H<sub>2</sub>O molecule is isolated in D<sub>2</sub>O, and address how the intramolecular coupling (between the two OH groups as well as with the intramolecular bending mode) and intermolecular coupling to translational modes depend on the shape of the local H-bond network. Although such information is not available in measurements on bulk water, it can be obtained by exploiting the properties of size-selected and cryogenically cooled water clusters, a regime that

has proven to be useful in the elucidation of the molecular-level mechanics underlying bulk behavior in a variety of contexts (11–24). This dataset provides a direct window into the degree to which excited-state dynamics contribute to the structure of the diffuse spectrum.

We specifically report the spectral signatures of individual H2O molecules located in each of the many spectroscopically distinct sites available in the  $Cs^+\cdot (H_2O)(D_2O)_{19}$  cluster ion [hereafter denoted Cs<sup>+</sup>(2H,38D)]. This system was selected because it adopts an arrangement in which the spherical Cs+ cation is encapsulated in a distorted pentagonal dodecahedral (PD) structure (25-27) at low temperature ( $\sim$ 20 K). The reported minimum-energy structure (26) of this cluster [computed with Gaussian 09 (28) at the B3LYP/6-31++G\*\* level of theory and basis with the LANL2DZ pseudopotential for Cs], hereafter denoted PDo, is depicted in Fig. 1. To best visualize this cage arrangement, a rotating PDF is available at the bottom of Fig. 1 and a larger version is provided in fig. S1, which reveals a twodimensional sheet of networked water molecules, each in a three-coordinate H-bonding configuration. There are two general classes of H-bonding environments that we classify as AAD and ADD configurations according to the number of acceptor (A) and donor (D) hydrogen bonds, respectively. The AAD class (red in Fig. 1) is distinguished by the free OH group (F<sub>OH</sub>) that projects out from the surface, whereas the ADD motif (orange) is embedded roughly in the plane of the surface.

The vibrational spectra of these size-selected cluster ions were obtained with a triple-focusing, cryogenic photofragmentation mass spectrometer described in detail previously (29) and briefly summarized in the supplementary materials. Spectra are obtained by monitoring infrared (IR) photoevaporation of weakly bound  $D_2$  molecules in a linear action regime, which is equivalent to absorption spectra (30).



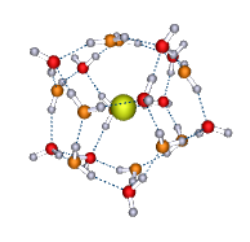


Fig. 1. Minimum-energy structure (26) of the distorted pentagonal dodecahedron (PD) cage formed by the Cs<sup>+</sup>-(H<sub>2</sub>O)<sub>20</sub> cluster, denoted PD<sub>0</sub>. On the top is a static picture of the PD<sub>0</sub> structure, and on the bottom is an interactive 3D model, which can be rotated in Adobe Reader. This structure has two classes of network sites (AAD, red; and ADD, orange) that differ by the number of H-bond acceptors (A) and donors (D) associated with the water molecules at each location.

The spectrum of the D<sub>2</sub>-tagged Cs<sup>+</sup>(40H) cluster (Fig. 2C) consists of a dense series of overlapping transitions that have been discussed previously (31). Highest in energy, the sharp feature at 3704 cm<sup>-1</sup> arises from the free OH group, and its location establishes that only AAD water molecules are present. This is clear because AD sites have been observed in other cluster sizes (32) and are indicated by a higher-energy transition appearing in the range 3710 to 3720 cm<sup>-1</sup>. Although the selection rules for IR activity are different than those at play in vibrational sum frequency generation (SFG) at the air-water interface (33) and at the surface of bulk (173 K) ice (34), it is useful to compare the vibrational patterns, with representative SFG spectra presented in Fig. 2, A and B, for ice and water, respectively (33, 34). The  $F_{OH}$  feature is evident in all the spectra. However, even though the ice surface, like the PD cluster, is dominated by equal contributions from ADD and AAD sites (35) (exactly 10 each for the PD structure), the cluster spectra are actually closer to that of the liquid water surface, where the envelope of the lower-energy band extends farther toward the free OH feature. For example, the  $\delta$ 

<sup>&</sup>lt;sup>1</sup>Sterling Chemistry Laboratory, Yale University, New Haven, CT 06520, USA. <sup>2</sup>Department of Chemistry, University of Washington, Seattle, WA 98195, USA.

<sup>\*</sup>Corresponding author. Email: mark.johnson@yale.edu (M.A.J.); abmccoy@uw.edu (A.B.M.)

feature in the air-water SFG spectrum at 3200 cm<sup>-1</sup> has been attributed to activity involving the bend overtone (33), where a prominent peak (b<sub>6</sub>) is observed in the cluster spectrum at 3191 cm<sup>-1</sup>. At the same time there are notable differences; the dominant feature in the Cs<sup>+</sup>(40H) cluster spectrum (Fig. 2C) occurs as a strong doublet (b<sub>1</sub>, b<sub>2</sub>) centered at 3554 cm<sup>-1</sup>, whereas the SFG response of both phases near 3554 cm<sup>-1</sup> is very weak.

The extensive range of the OH stretching bands in the Cs<sup>+</sup>(40H) spectrum arises in part from the very large number of nearly equivalent PD structures. However, even for a single representative structure (PD $_0$  in Fig. 1) (36, 37), the calculated harmonic spectrum (fig. S2) indicates that the frequency of a given H-bonded OH oscillator depends not only on the site class (ADD versus AAD), but also on the hydrogen bonding arrangements of the molecules surrounding it (38, 39). For example, the transition associated with the donor OH group is predicted to be much less redshifted when the acceptor water molecule has a free OH group. This effect has been treated in neutral water clusters by Ohno et al. (38) and later extended to the liquid, ice, and interface regimes by Tainter et al. (39) When these extended patterns are included, the PDo structure is quite asymmetrical such that essentially all the bound OH groups are in topologically distinct environments. As a result, the calculated fundamentals (displayed in fig. S2) are distributed over 600 cm<sup>-1</sup>, and harmonic analysis of the bands arising from the various sites in the PD<sub>0</sub> structure indicates a strong correlation between the redshift of a given site and the H-bonding index advocated by Skinner and co-workers (39), as illustrated in figs. S2B and S3.

We next describe how the local PD network sites that contribute to the pattern in Fig. 2C can be revealed by using an isotopic labeling scheme that is only available in the cluster regime. Specifically, because chemical scrambling between the OH and OD groups is strongly suppressed in water clusters, a single, intact H<sub>2</sub>O molecule can be incorporated into an otherwise perdeuterated assembly (40, 41). Consequently, an H<sub>2</sub>O molecule can be integrated into the PD cage by ligand exchange, a process in which preformed Cs<sup>+</sup>·(D<sub>2</sub>O)<sub>20</sub> clusters interact at low pressure with H<sub>2</sub>O vapor as described in the supplementary materials. This mechanism is verified by the absence of the HDO bending fundamental in the spectra of clusters with the stoichiometry  $Cs^+\cdot (H_2O)(D_2O)_n$  (40) and the suppression of odd numbers of H atoms in the product ion isotopologs (see mass spectrum in fig. S4), which would reveal chemical scrambling by evaporation of HDO.

The vibrational spectrum of the D2-tagged Cs<sup>+</sup>(2H,38D) isotopolog is compared in Fig. 2D with that of Cs<sup>+</sup>(40H) in Fig. 2C. The overall envelope of the Cs<sup>+</sup>(2H,38D) covers the energy range observed for the Cs<sup>+</sup>(40H) cluster, with the positions of the labeled peaks collected in tables S1 and S2. Because only two OH oscillators are available in the mass-selected Cs<sup>+</sup>(2H.38D) ion, the extent of its OH stretching region must arise from H<sub>2</sub>O occupation of many different

sites within the PD structure to create a plethora of isotopomers. One important difference in the spectra of the two isotopologs is that the free OH feature in the Cs<sup>+</sup>(2H,38D) spectrum is clearly enhanced relative to that in the Cs<sup>+</sup>(40H) cluster, indicating that the free OH site is preferentially populated in the cold ensemble. This is consistent with the behavior observed at the surface of water, where nuclear quantum effects strengthen the bonds holding D2O molecules in ADD sites (42). The similarities in the band shapes in Fig. 2, C and D, raise the question of whether the spectrum of the homogeneous isotopolog is a simple superposition of the spectra of isolated H<sub>2</sub>O molecules occupying the various sites, or reflects coupling among nearby molecules in the PD structure. Indeed, the only major differences between the two spectra are the character of the absorptions near 3350 cm<sup>-1</sup> (a<sub>4</sub> versus b<sub>4</sub> in Fig. 2, C and D), a 14 cm<sup>-1</sup> redshift in the strong doublet  $(a_1, a_2 \text{ versus } b_1, b_2 \text{ in Fig. 2D})$  below the free OH feature at  $\sim$ 3700 cm<sup>-1</sup>, and a small (<10 cm<sup>-1</sup>) redshift in the a<sub>6</sub>-b<sub>6</sub>, a<sub>7</sub>-b<sub>7</sub> features at the lower energy region of the absorption. To put this in context, the matrix elements arising from intermolecular coupling have been considered for bulk water (1) and found to display a broad distribution with a maximum value of 28 cm<sup>-1</sup>, depending on the orientations and fundamental OH stretching frequencies of the nearby water molecules. This coupling was explored at the harmonic level with the methods developed by Sibert and co-workers (24), which involves decoupling the various OH oscillators that make up the normal modes of the PD<sub>o</sub> structure (43). The results of this analysis are provided in table S3 and indicate that, for the AAD molecules, the couplings range from 33 to 45 cm<sup>-1</sup>, which lead to ~5 cm<sup>-1</sup> shifts in the frequencies of the OH stretching fundamentals.

Provided that the Cs<sup>+</sup>(2H,38D) clusters are sufficiently cold to suppress spontaneous interconversion between the isotopomers that differ according to site occupation by H<sub>2</sub>O, the spectrum is a heterogeneous superposition of their distinct spectra. As such, isotopomer-specific spectra provide a direct way to extract the spectrum of an H<sub>2</sub>O molecule located in each site. Of particular importance, these spectra reveal the embedded correlations between transitions derived from the two OH groups that are distributed throughout the ensemble spectrum. We isolated the site-specific spectra using a two-color, IR-IR photobleaching approach described elsewhere (29). This requires three stages of mass selection and is therefore denoted a MS<sup>3</sup>IR<sup>2</sup> class of secondary analysis. In this application, one IR laser is fixed on a particular probe transition while another, powerful IR laser is scanned through the entire spectrum. The photofragment yield from the probe laser then reveals the isotopomer-selective spectrum as a series of dips as the pump laser removes population from the species selected by the probe frequency.

Figure 3B demonstrates how the MS<sup>3</sup>IR<sup>2</sup> approach can establish the locations of the transitions arising from the bound OH companion of the free OH group on the same water molecule. This is accomplished by fixing the probe laser on

the free OH band at 3699 cm<sup>-1</sup> (a<sub>0</sub>) while the pump laser is scanned across the OH region. The resulting dip spectrum (Fig. 3B) exhibits a very large gap between the  $F_{OH}$  band and the onset of a diffuse absorption envelope below 3400 cm<sup>-1</sup>. This observation provides direct evidence that the bands in the lower-energy region of the spectrum (a<sub>4-7</sub>) are exclusively due to excitation of the bound OH group associated with H<sub>2</sub>O molecules

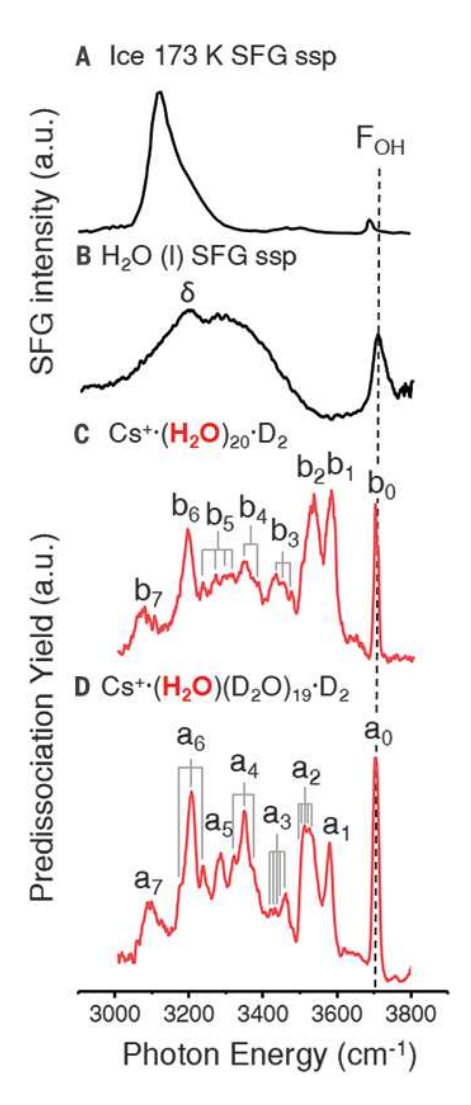


Fig. 2. Comparison of SFG spectra from the ice and liquid water surfaces with the experimental vibrational spectra of Cs<sup>+</sup>(40H)·D<sub>2</sub> and its isotopolog incorporating an intact H<sub>2</sub>O molecule. SFG spectra of ice-vapor (A) (34) and water-air (B) (33) interfaces [reproduced with permission from (33) by the American Chemical Society and (34) by the American Physical Society] obtained by using ssp polarization combinations. (C and D) Spectra were obtained by predissociation of the (C)  $Cs^+ \cdot (H_2O)_{20} \cdot D_2$ , and (D)  $Cs^+ \cdot (H_2O)(D_2O)_{19} \cdot D_2$  cluster ions. The δ label indicates assignment of the intramolecular HOH bending overtone from (33). The frequencies of features labeled an and bn are included in tables S1 and S2.

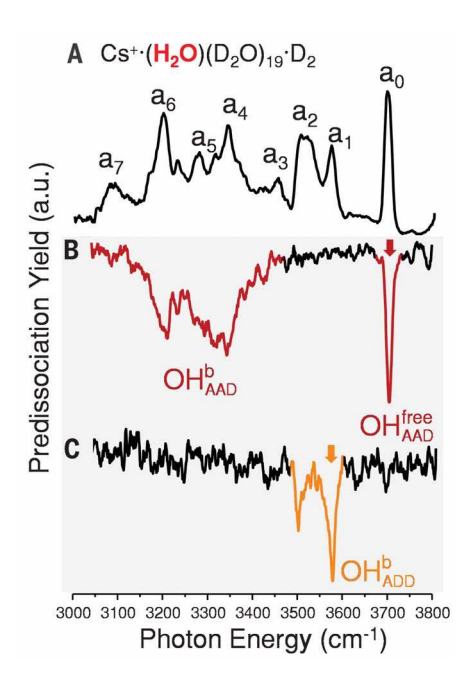


Fig. 3. Isolation of the contributions of the AAD (red) and ADD (orange) water molecules to the spectrum of the  $Cs^+(2H, 38D) \cdot D_2$  isotopolog. Vibrational predissociation spectrum of (A)  $Cs^+ \cdot (2H, 38D) \cdot D_2$  and two-color, IR-IR double resonance hole burning spectra of  $Cs^+ \cdot (2H, 38D) \cdot D_2$  with the probe laser fixed on (B) the  $a_0$  (red arrow) and (C) the  $a_1$  (orange arrow) features, thus isolating the signatures of  $H_2O$  in AAD and ADD sites, respectively.

in AAD network sites. Consequently, the strong doublet (a<sub>1</sub> and a<sub>2</sub>) centered at 3540 cm<sup>-1</sup> must be exclusively derived from the ADD sites. That conclusion can again be directly tested, this time by fixing the probe laser on the dominant peak a<sub>1</sub> at 3573 cm<sup>-1</sup> to yield the dip spectrum in Fig. 3C, which indeed reveals two bands spaced by ~80 cm<sup>-1</sup>. The separation between these two transitions is consistent with the splitting between the two donor OH groups on the same molecule (44). Although the splitting is close to that (99 cm<sup>-1</sup>) found for the symmetric and antisymmetric stretches in an isolated water molecule, harmonic analysis of the couplings of the local OH oscillators in the PDo structure indicates that the leading contribution to the splitting comes from differences in the environment of the two OH bonds in the various ADD sites (see table S3). The traces in Fig. 4, B and C, display how this doublet evolves in the region of the  $a_1$ - $a_3$  peaks, demonstrating that these distinct ADD contributions are partially overlapping.

The overall behavior displayed in Fig. 3 is in qualitative agreement with the harmonic prediction (fig. S2) that the AAD and ADD classes contribute to distinct regions of the spectrum. We next address the nature of the free OH feature and the diffuse absorption displayed by the AAD sites below 3400 cm<sup>-1</sup> in the Cs<sup>+</sup>(2H,38D) spectrum (Fig. 3B). Because all AAD sites necessarily display a free OH feature, further isolation of the

independent contributions to the low-energy envelope must be accomplished by probing various locations (indicated by purple arrows in Fig. 4, E to H) throughout the region. As expected, all these probe positions yield a free OH band, but the isotopomer-selective spectra reveal that the feature near 3700 cm<sup>-1</sup> is actually heterogeneous. Specifically, there are two even narrower [~9 cm<sup>-1</sup> full width at half maximum (FWHM)] components to this feature, as highlighted by the expanded scan in fig. S5. The MS<sup>3</sup>IR<sup>2</sup> spectra in Fig. 4, E to H, establish that there are at least four distinct network sites contributing to the diffuse low-energy envelope (Fig. 3B). These scans display an evolving multiplet substructure as the probe energy approaches a narrower band (a<sub>6</sub>, blue) near 3200 cm<sup>-1</sup>. This narrow band appears near the expected location for the  $v = 0 \rightarrow 2$ overtone transition arising from the HOH bending fundamental ( $v_{HOH}$ ) at ~1600 cm<sup>-1</sup>, which is nominally IR forbidden in the double harmonic level approximation (i.e., normal modes coupled with a linear expansion of the dipole surface). It is well known (45) that the OH (v = 1) and  $(v_{HOH})$  (v = 2) harmonic states are often anharmonically coupled in a Fermi resonance interaction, which yields two mixed states that both contribute to the IR absorption spectrum. In the model commonly used (45) to treat this effect, the intensity ratio of the two transitions depends on the energy separation between the two unperturbed levels and the matrix element that couples them. Because the bending mode is relatively insensitive to local coordination, the overtone remains relatively fixed whereas the OH fundamentals are incrementally redshifted through the energy of the  $(v_{HOH})$  (v = 2) level. Although the spectrum in Fig. 4G appears to result from the overlap of at least two distinct contributions (as evidenced by the broadening of the  $F_{\rm OH}$  peak), the traces in Fig. 4, E and F, yield sharper  $F_{OH}$  bands and were therefore further analyzed to reveal the intramolecular coupling mechanics. The observed patterns were fit to a simple  $2 \times 2$  interaction picture in which the oscillator strength of the bend overtone occurs through intensity borrowing from the nearby OH (v = 1) level. This procedure indicates that Fermi coupling matrix elements of 40 and 53 cm<sup>-1</sup> are required to recover the observed patterns (solid lines in traces Fig. 4, E and F, respectively), with the width (FWHM) of the nominal OH stretching fundamental of about 60 cm<sup>-1</sup>, as illustrated in detail in fig. S6. This matrix element is larger than that (~33 cm<sup>-1</sup>) reported earlier in the X<sup>-</sup>·H<sub>2</sub>O (X, halide) systems (45). The width associated with the bound OH group is also of interest, as it establishes an excited state relaxation time of the OH oscillator on the order of 200 fs. Equally important is the observation that these broadened bands occur without appreciable excitation of combination bands involving low-frequency intermolecular vibrational modes (46), unlike the situation encountered in the microhydration of anions (29).

We have established that the range of frequencies exhibited by the OH oscillators of  $H_2O$  molecules occupying seven distinct sites in the  $Cs^+\cdot (H_2O)_{20}$  cluster covers the same region that

is found in the SFG spectrum of the air-water interface. We further demonstrated how, by following the spectroscopic behavior of single (intact) H<sub>2</sub>O molecules embedded in the pentagonal dodecahedron water cage surrounding the Cs<sup>+</sup> cation, we can unmask previously hidden mechanistic features that underlie the diffuse IR spectrum of the tri-coordinated, two-dimensional water network. The water molecules that are embedded in the cage surface by donating two H-bonds to neighbors exclusively account for the absorption in the range 3450 to 3600 cm<sup>-1</sup>, whereas the bound OH companion of water molecules with a free OH group yield all of the more diffuse absorption below 3450 cm<sup>-1</sup>. The v = 1 level of the OH stretching manifold associated with that bound OH group undergoes a

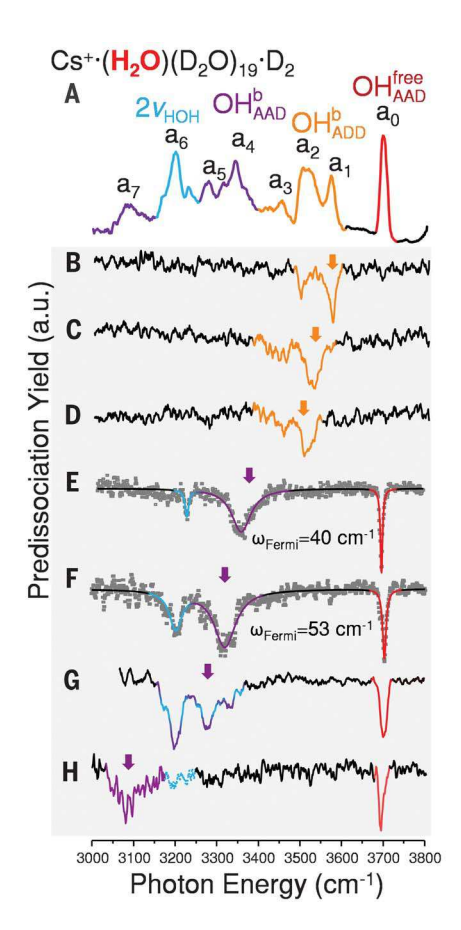


Fig. 4. Isolation of band patterns associated with spectroscopically distinct sites occupied by an intact H<sub>2</sub>O molecule in the Cs<sup>+</sup>(2H,38D)·D<sub>2</sub> cluster, obtained by fixing the probe laser at the photon energies indicated by downward arrows while scanning the pump laser through the OH stretching region. (A) Nonselective predissociation spectrum of Cs<sup>+</sup>(2H,38D)·D<sub>2</sub>, (B to D) bands due to ADD sites (orange), and (E to H) bands arising from AAD sites. The AAD contributions are further resolved into excitations of free OH (red), bound OH (purple), and intramolecular bend overtones (blue). The solid lines in (E) and (F) are fits to a  $2 \times 2$  coupling scheme between the OH stretch and intramolecular bend described in detail in fig. S6.

strong Fermi type interaction with the v = 2 level of the intramolecular HOH bending mode as the former is redshifted through the zero-order location of the bend overtone near ~3200 cm<sup>-1</sup> with a matrix element of ~45 cm<sup>-1</sup>. These results establish the intrinsic breadths and multiplet signatures associated with excitation of a water molecule at very low temperature, which must result from anharmonic couplings among the excited vibrational states. With this information and experimental capability in hand, an exciting direction for future work will be to follow the onset of spectral diffusion in microcanonical ensembles and thus reveal the trajectories of the large-amplitude motions that underlie the rapid spectral diffusion exhibited by bulk water.

#### **REFERENCES AND NOTES**

- B. M. Auer, J. L. Skinner, J. Chem. Phys. 128, 224511 (2008).
- 2. H. J. Bakker, J. L. Skinner, Chem. Rev. 110, 1498-1517 (2010).
- F. Perakis et al., Chem. Rev. 116, 7590-7607 (2016).
- T. Hayashi, T. la Cour Jansen, W. Zhuang, S. Mukamel,
- J. Phys. Chem. A 109, 64-82 (2005). S. A. Corcelli, C. P. Lawrence, J. L. Skinner, J. Chem. Phys. 120,
- 8107-8117 (2004).
- T. Steinel et al., Chem. Phys. Lett. 386, 295-300 (2004).
- A. Bankura, A. Karmakar, V. Carnevale, A. Chandra, M. L. Klein, J. Phys. Chem. C 118, 29401-29411 (2014).
- 8. A. Paarmann, T. Havashi, S. Mukamel, R. J. D. Miller. J. Chem. Phys. 130, 204110 (2009).
- L. De Marco, J. A. Fournier, M. Thämer, W. Carpenter, A. Tokmakoff, J. Chem. Phys. 145, 094501 (2016).
- 10. D. F. Hornig, H. F. White, F. P. Reding, Spectrochimica Acta 12, 338-349 (1958)
- 11. N. I. Hammer et al., Science 306, 675-679 (2004).
- 12. R. M. Young, D. M. Neumark, Chem. Rev. 112, 5553-5577 (2012).
- 13. B. Abel, U. Buck, A. L. Sobolewski, W. Domcke, Phys. Chem. Chem. Phys. 14, 22-34 (2012).
- 14. C. T. Wolke et al., Science 354, 1131-1135 (2016).
- 15. J. A. Fournier et al., Science 344, 1009-1012 (2014).

- 16. F. N. Keutsch, R. J. Saykally, Proc. Natl. Acad. Sci. U.S.A. 98, 10533-10540 (2001).
- 17. J. D. Smith et al., Science 306, 851-853 (2004).
- 18. W. T. S. Cole et al., J. Chem. Phys. 148, 094301 (2018).
- 19. W. T. S. Cole, R. J. Saykally, J. Chem. Phys. 147, 064301 (2017).
- 20. C. Pérez et al., Science 336, 897-901 (2012).
- 21. C. Pérez et al., Angew. Chem. Int. Ed. 53, 14368-14372 (2014).
- 22. J. R. Clarkson et al., Science 307, 1443-1446 (2005). 23. J. R. Clarkson, J. M. Herbert, T. S. Zwier, J. Chem. Phys. 126,
- 134306 (2007). 24. D. P. Tabor, R. Kusaka, P. S. Walsh, T. S. Zwier, E. L. Sibert 3rd, J. Phys. Chem. A 119, 9917-9930 (2015).
- 25. R. J. Cooper, T. M. Chang, E. R. Williams, J. Phys. Chem. A 117, 6571-6579 (2013).
- 26. F. Schulz, B. Hartke, ChemPhysChem 3, 98-106 (2002).
- 27. A. Selinger, A. W. Castleman, J. Phys. Chem. 95, 8442-8444
- 28. Gaussian 09, M. J. Frisch et al., (Gaussian, Inc., Wallingford, CT. 2009)
- 29. N. Yang, C. H. Duong, P. J. Kelleher, M. A. Johnson, A. B. McCoy, Chem. Phys. Lett. 690, 159-171 (2017).
- 30. A. B. Wolk, C. M. Leavitt, E. Garand, M. A. Johnson, Acc. Chem. Res. 47, 202-210 (2014).
- 31. J. A. Fournier et al., Proc. Natl. Acad. Sci. U.S.A. 111, 18132-18137 (2014).
- 32. M. Miyazaki, A. Fujii, T. Ebata, N. Mikami, Science 304, 1134-1137 (2004).
- 33. J. Schaefer, E. H. G. Backus, Y. Nagata, M. Bonn, J. Phys. Chem. Lett. 7, 4591-4595 (2016).
- 34. X. Wei, P. B. Miranda, C. Zhang, Y. R. Shen, Phys. Rev. B 66, 085401 (2002).
- 35. W. J. Smit et al., Phys. Rev. Lett. 119, 133003 (2017).
- 36. F. Schulz, B. Hartke, Phys. Chem. Chem. Phys. 5, 5021-5030 (2003).
- 37. D. J. Anick, J. Chem. Phys. 132, 164311 (2010).
- 38. K. Ohno, M. Okimura, N. Akai, Y. Katsumoto, Phys. Chem. Chem. Phys. 7, 3005-3014 (2005).
- 39. C. J. Tainter, Y. Ni, L. Shi, J. L. Skinner, J. Phys. Chem. Lett. 4, 12-17 (2013).
- 40. C. T. Wolke et al., J. Chem. Phys. 144, 074305 (2016).
- 41. A. S. Zatula, M. J. Ryding, P. U. Andersson, E. Uggerud, Int. J. Mass Spectrom. 330-332, 191-199 (2012).
- 42. Y. Nagata, R. E. Pool, E. H. G. Backus, M. Bonn, Phys. Rev. Lett. 109, 226101 (2012).

- 43. L. C. Dzugan, R. J. DiRisio, L. R. Madison, A. B. McCoy, Faraday Discuss. 212, 443-466 (2018).
- 44. S. M. Gruenbaum, C. J. Tainter, L. Shi, Y. Ni, J. L. Skinner, J. Chem. Theory Comput. 9, 3109-3117 (2013).
- 45. W. H. Robertson, G. H. Weddle, J. A. Kelley, M. A. Johnson, J. Phys. Chem. A 106, 1205-1209 (2002).
- 46. S. M. Craig et al., Proc. Natl. Acad. Sci. U.S.A. 114, E4706-E4713 (2017).

### **ACKNOWLEDGMENTS**

We thank J. K. Denton, H. J. Zeng, S. Mitra, and E. H. Perez for technical assistance in the experimental enhancements necessary to achieve the signal to noise required to obtain these measurements. Additionally, we thank D. Anick for discussions regarding the presence of various structural isomers of the Cs<sup>+</sup>(H<sub>2</sub>O)<sub>20</sub> at low temperatures. Funding: M.A.J. thanks the National Science Foundation under grant CHE-1465100 for funding the research on the Cs<sup>+</sup> water clusters and the Air Force Office of Scientific Research under DURIP grant FA9550-17-1-0267 for funding the two-color, IR-IR tandem time-of-flight mass spectrometry instrument. C.H.D. thanks the National Science Foundation Graduate Research Fellowship for funding under grant DGE-1122492. A.B.M. thanks the National Science Foundation under grant CHE-1619660. Parts of this work were performed using the Ilahie cluster, which was purchased with funds from an MRI grant from the National Science Foundation (CHE-1624430). Author contributions: M.A.J. conceptualized and supervised the research; N.Y., C.H.D., P.J.K., A.B.M., conducted the investigation and formal analysis; N.Y., C.H.D., P.J.K., built the instrument and lasers used in this experiment; N.Y., A.B.M., M.A.J. wrote the original draft; N.Y., C.H.D., P.J.K., A.B.M., M.A.J., reviewed and edited the subsequent drafts. Competing interests: The authors declare no conflicts of interest. Data and materials availability: Data tabulating each spectral trace are available in the supplementary materials as Data S1.

### SUPPLEMENTARY MATERIALS

science.sciencemag.org/content/364/6437/275/suppl/DC1 Materials and Methods

Figs S1 to S6 Tables S1 to S3 Data S1

18 December 2018; accepted 11 March 2019 10.1126/science.aaw4086



## Deconstructing water's diffuse OH stretching vibrational spectrum with cold clusters

Nan Yang, Chinh H. Duong, Patrick J. Kelleher, Anne B. McCoy and Mark A. Johnson

Science **364** (6437), 275-278. DOI: 10.1126/science.aaw4086

Wet surface sightings in clusters

In principle, the surface structure of water (H<sub>2</sub>O) should be discernable from the O–H vibrations. In practice, however, so many configurations rapidly interconvert that the bands are bewilderingly broad. Yang *et al.* studied a cluster of 20 H <sub>2</sub>O surrounding a cesium ion, using isotopomers that vary in the position of one H<sub>2</sub>O amid 19 heavy water (D <sub>2</sub>O) molecules. Precisely assigned spectral features from contributing configurations mapped well onto a bulk surface spectrum.

Science, this issue p. 275

ARTICLE TOOLS http://science.sciencemag.org/content/364/6437/275

SUPPLEMENTARY http://science.sciencemag.org/content/suppl/2019/04/17/364.6437.275.DC1 MATERIALS

**REFERENCES** This article cites 45 articles, 9 of which you can access for free

http://science.sciencemag.org/content/364/6437/275#BIBL

PERMISSIONS http://www.sciencemag.org/help/reprints-and-permissions

Use of this article is subject to the Terms of Service